Electronic Supplimentary Information

Highly dual-doped multilayer nanoporous graphene: efficient metal-free electrocatalysts for hydrogen evolution reaction

Hongliang Jiang, Yihua Zhu,* Yunhe Su, Yifan Yao, Yanyan Liu, Xiaoling Yang and Chunzhong Li

Key Laboratory for Ultrafine Materials of Ministry of Education, School of Materials Science and Engineering, East China University of Science and Technology, Shanghai 200237, China.

*Corresponding author: Fax: +86-21-64250624; yhzhu@ecust.edu.cn (Y. Zhu)

Experimental Section

Materials. Urea, phosphoric acid (H_3PO_4) and glucose were purchased from Shanghai Lingfeng Chemical Reagent Co. Ltd. Nafion (5 wt%) was obtained from Sigma-Aldrich. Pt/C (20 wt%) was obtained from Johnson-Matthey. All chemicals are of analytical grade and used as received. Ultrapure water (18 MΩ·cm) was used for all experiments.

Synthesis of highly dual-doped multilayer nanoporous graphene. The nitrogen and phosphorus dual-doped multilayer nanoporous graphene was prepared by a facile one-step heating approach. In a typical procedure, urea (10 g), glucose (0.5 g), and phosphoric acid (0.2 g) were dissolved in deionized water (100 mL) and stirred at 80 °C to remove water. The resulting white powder was transferred into a crucible, heated at a rate of 3 °C min^{-1} to an appointed temperature and maintained at that temperature for 2 h. Afterwards, the sample was allowed to cool naturally to room temperature and then conducted ultrasonic exfoliation process. All the annealing and cooling processes were carried out under argon flow. Three annealing temperature of 800, 900, and 1000 °C were chosen to synthesize NPG800, NPG900 and NPG1000, respectively. The only nitrogen-doped nanoporous graphene (NG900) was prepared by a similar process without adding phosphoric acid.

Characterization. The morphology and microstructure of all samples were examined by High-transmission electron microscopy (TEM: JEM-2100, operated at 200kV), Scanning electron microscopy (FE-SEM: S-4800) and Atomic force microscopy (AFM: Veeco Dimension 3100). The specific surface area, pore volume, and pore size of samples were investigated by Bruauer-Emmett-Teller (BET) and Barrett-Joyner-Halenda (BJH) models. X-ray diffractometer (XRD: D/Max2000, Rigaku) was used for powder analysis. Raman spectra were recorded with a Bruker RFS 100/S spectrometer to analyze the degree of graphitization of the carbon. X-ray photoelectron spectroscopy (XPS: VG ESCA 2000 with an Mg Kα as source and the C1s peak at 284.6 eV as an internal standard) was used to demonstrate the content of carbon, nitrogen and phosphorus and the doping types of the latter two elements.

Electrochemical measurements. Electrochemical measurements were performed at room temperature using a rotating disk working electrode made of GC (PINE, 5 mm diameter, 0.196 cm^2) connected to a computer-controlled CHI660C advanced electrochemical system with a conventional three-electrode cell. An Ag/AgCl (3.0 M KCl) electrode and a Pt wire electrode were used as reference electrode and counter electrode, respectively. A glassy carbon (GC) electrode for working electrode was polished using 0.3 and 0.05 μm alumina slurries followed by washing with water and acetone. 4 mg of as-prepared samples (or Pt/C) and 80 μL Nafion solution (5 wt%) were dissolved in 1 mL of water by sonication to obtain a homogeneous black suspension solution. 10 μL of as-obtained solutions were pipetted onto a GC electrode surface and dried at room temperature (this gave a catalyst loading of ~0.20 mg cm^{-2}). A flow of N_2 was maintained over the electrolyte during the experiment to eliminate dissolved oxygen. The working electrode was rotated at 1600 rpm to remove hydrogen gas bubbles formed at the catalyst surface. The electrocatalytic activity of the catalysts towards HER was examined by polarization curves using linear sweep voltammetry (LSV) with a scan rate of 2 mV s^{-1} in 0.5 M H_2SO_4 at room temperature. The polarization curves were replotted as overpotential (η) vs log current (log j) to get Tafel plots for assessing the HER kinetics of investigated catalysts. By fitting the linear portion of the Tafel plots to the Tafel equation ($\eta = b \log (j) + \alpha$), the Tafel slope ($b$) can be obtained. All polarization curves were corrected for the iR contribution within the cell. All of the potentials in our manuscript were

calibrated to a reversible hydrogen electrode (RHE).

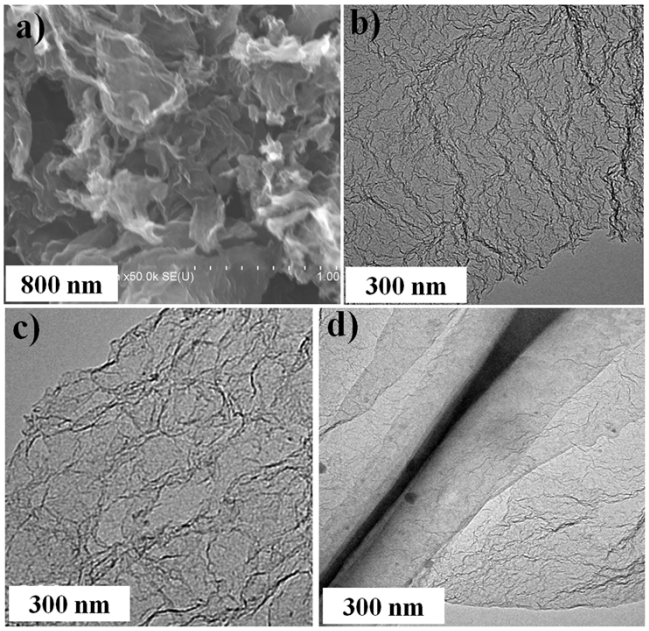

Figure S1. SEM image of (a) the NPG900 and TEM images of (b) the NPG800, (c) the NPG1000, and (d) the NG900.

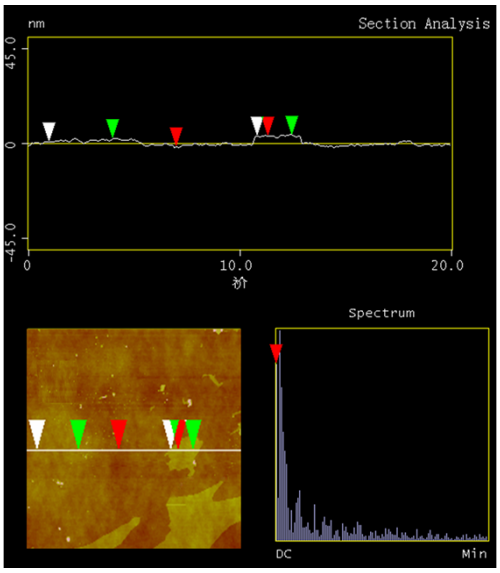

Figure S2. AFM image of the NPG900.

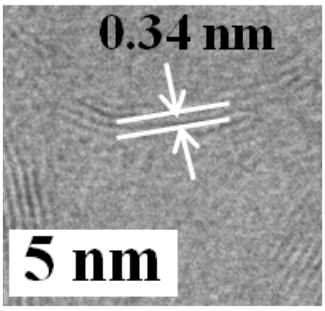

Figure S3. The HRTEM images of the NPG900.

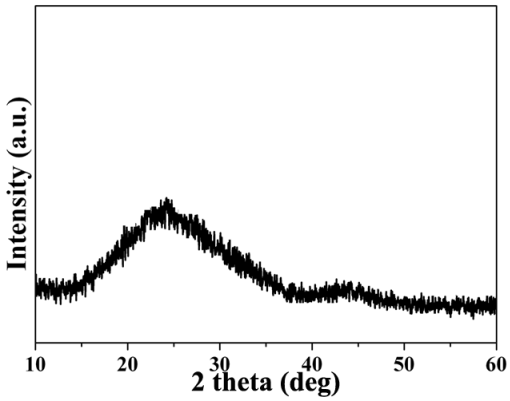

Figure S4. XRD pattern of the NPG900.

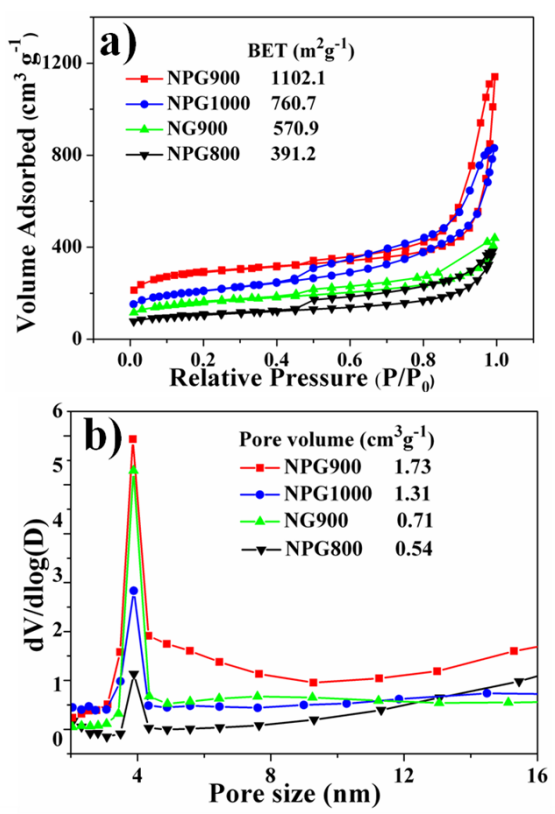

Figure S5. N_2 adsorption–desorption isotherms and the corresponding pore size distribution (inset) of all samples.

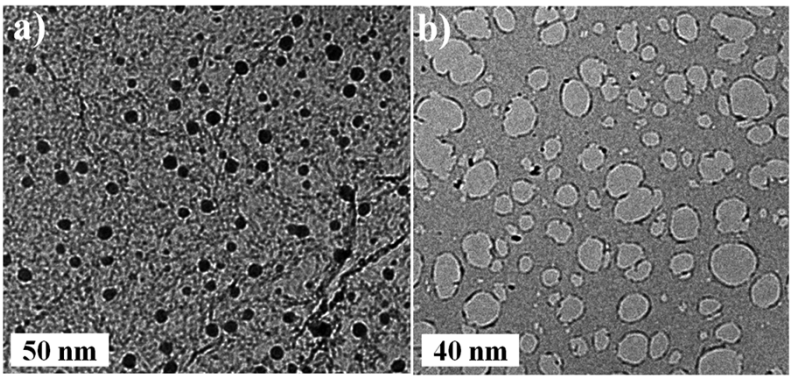

Figure S6. the TEM images of NPG samples before (a) and after (b) ultrasonic exfoliation.

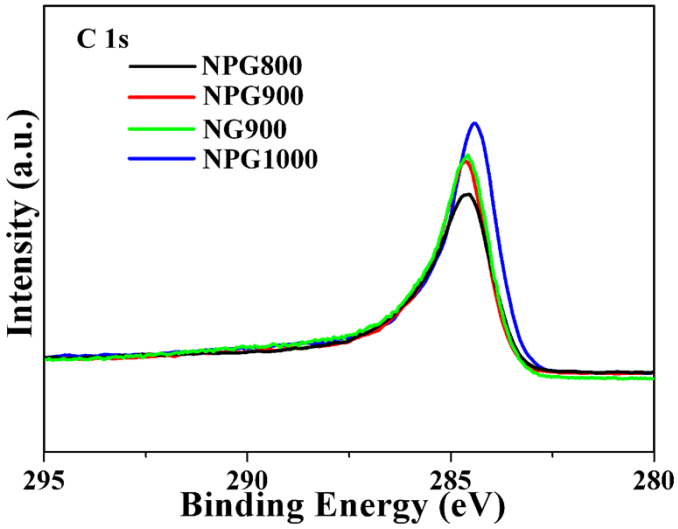

Figure S7. C1s spectra of all samples.

Table S1. Atomic percents (at. %) of C, N, P, and O of all samples from XPS analysis.

Samples	C content (at. %)	N content (at. %)	P content (at. %)	O content (at. %)
NPG800	68.2	13.2	3.1	15.7
NPG900	72.1	11.3	2.9	13.7
NPG1000	80.2	7.3	2.3	10.2
NG900	75.5	10.7	0	13.8

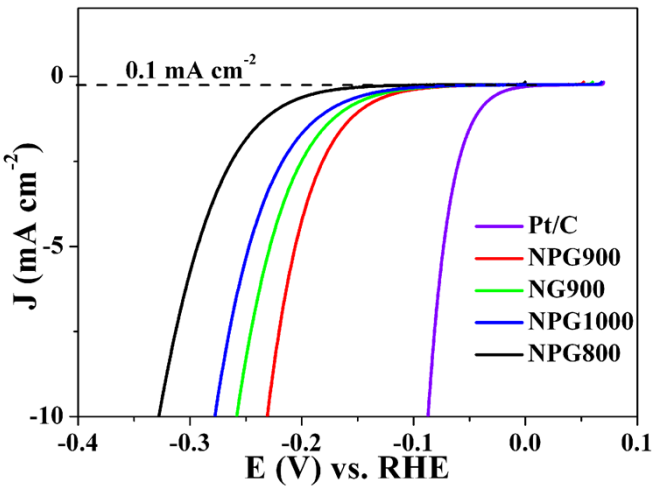

Figure S8. Polarization curves of all samples in 0.5 mM H_2SO_4.

Table S2. Onset overpotentials, Tafel slopes, Exchange current density and operating potential at 10 mA cm^{-2} of all samples.

Samples	Onset overpotentials (V) at J = 0.1 mA cm^{-2}	Tafel slope (mV/dec)	Exchange current density (mA cm^{-2})	η (mV) at J = 10 mA cm^{-2}
NPG800	0.17	100	0.0086	381
NPG900	0.12	79	0.0243	213
NPG1000	0.14	94	0.0239	238
NG900	0.13	92	0.0241	258
Pt/C	0	35	0.6910	67

Table S3. Onset overpotentials, Tafel slopes, Exchange current density and operating potential at 10 mA cm^{-2} of noble-metal-free materials reported in the literature.

catalyst	Onset overpotentials (V) at J = 0.1 mA cm^{-2}	Tafel slope (mV/dec)	Exchange current density (mA cm^{-2})	η (mV) at J = 10 mA cm^{-2}	Ref.
MoS_2 ultrathin sheets	0.15	50	0.0089	195	1
Lamellar $CoSe_2$ nanobelts	0.05	48	0.0084	115	2
Monolayer MoS_2 supported by NPG	0.12	46	0.0004	226	3
MoO_3/MoS_2 nanowires	0.15~0.20	50~60	N/A	240	4
FeP nanosheets	0.1	67	N/A	N/A	5
N,P-doped graphene	0.29	91	0.0003	420	6
C_3N_4@N-doped graphene	N/A	51	0.0004	240	7
Activated carbon nanotubes	0.10	71	0.016	N/A	8
NS co-doped graphene 500C	0.13	81	0.0084	276	9
NPG900	0.12	79	0.0243	213	This work
NPG1000	0.14	94	0.0239	238	This work
NG900	0.13	92	0.0241	258	This work
NPG800	0.17	100	0.0086	381	This work

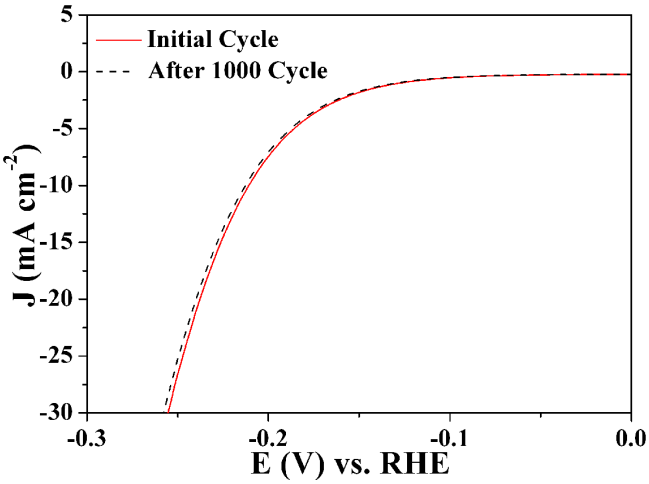

Figure S9. Cycle stability of NPG900.

References:

1. J. Xie, H. Zhang, S. Li, R. Wang, X. Sun, M. Zhou, J. Zhou, X. Lou and Y. Xie, *Adv. Mater.*, 2013, **25**, 5807.

2. Y. Xu, M. Gao, Y. Zheng, J. Jiang and S. Yu, *Angew. Chem. Int. Ed.*, 2013, **52,** 8546.

3. Y. Tan, P. Liu, L. Chen, W. Cong, Y. Ito, J. Han, X. Guo, Z. Tang, T. Fujita, A. Hirata and M. Chen, *Adv. Mater.*, 2014, **26**, 8023.

4. Z. Chen, D. Cummins, B. Reinecke, E. Clark, M. Sunkara and T. Jaramillo, *Nano Lett.*, 2011, **11,** 4168.

5. Y. Xu, R. Wu, J. Zhang, Y. Shi and B. Zhang, *Chem. Commun.*, 2013, **49,** 6656.

6. Y. Zheng, Y. Jiao, L. Li, X. Tan, Y. Chen, M. Jaroniec and S. Qiao, *ACS Nano*, 2014, **8**, 5290.

7. Y. Zheng, Y. Jiao, Y. Zhu, L. Li, Y. Han, Y. Chen, A. Du, M. Jaroniec and S. Qiao, *Nat. Commun.*, 2014, **5**, 3783.

8. W. Cui, Q. Liu, N. Cheng, A. Asiri and X. Sun, *Chem. Commun.*, 2014, **50**, 9340.

9. Y. Ito, W. Cong, T. Fujita, Z. Tang and M. Chen, *Angew. Chem. Int. Ed.*, 2015, **54**, 2131.